Transient Plasma Photonic Crystals for High-Power Lasers

G. Lehmann and K. H. Spatschek
Institut für Theoretische Physik I, Heinrich-Heine-Universität Düsseldorf, D–40225 Düsseldorf, Germany
(Received 25 February 2016; published 2 June 2016)

A new type of transient photonic crystals for high-power lasers is presented. The crystal is produced by counterpropagating laser beams in plasma. Trapped electrons and electrically forced ions generate a strong density grating. The lifetime of the transient photonic crystal is determined by the ballistic motion of ions. The robustness of the photonic crystal allows one to manipulate high-intensity laser pulses. The scheme of the crystal is analyzed here by 1D Vlasov simulations. Reflection or transmission of high-power laser pulses are predicted by particle-in-cell simulations. It is shown that a transient plasma photonic crystal may act as a tunable mirror for intense laser pulses. Generalizations to 2D and 3D configurations are possible.

DOI: 10.1103/PhysRevLett.116.225002

Photonic crystals are one- ore multidimensional periodic structures with a periodicity length of the order of an optical wavelength. Photonic band structures [1] are analogues to electronic bands. They also show frequency bands (photonic band gaps) of inhibited optical modes. Research work on photonic crystals started several decades ago with the pioneering works of Yablonovitch [2] and John [3]. The names "photonic crystal" and "photonic band gap" were introduced in 1989 by Yablonovitch and Gmitter [4]. Since then, new science has emerged at the interface between condensed-matter physics and photonics, and a range of technological developments became possible [5–7]. Slow light in photonic crystals is a promising solution for buffering and time-domain processing of optical signals [8]. Nonlinear photonic crystals may bring to reality the vision of light controlling by light comparable to electronics, where electrons control electrons [9]. Nonlinear frequency conversion with applications to second-harmonic generation and multiple wavelength frequency conversion were proposed [10]. Discrete solitons as self-trapped wave packets result from the interplay between lattice diffraction and material nonlinearity [11–15]. The idea of discrete optical components was further promoted via diffraction management [16] and modulated photonic lattices and waveguides [17,18].

In the present Letter, we investigate transient plasma photonic crystals when high-intensity laser light is controlling short pulse lasers. A plasma is used as the underlying medium, since otherwise for solids laser damage might occur [19]. The typical damage threshold fluence for silica is on the level of up to 10 J/cm^2 for pulse durations in the femtosecond to picosecond regime, whereas the fluences considered here are more than 5 orders of magnitude larger. The transient plasma photonic crystal (TPPC) being considered here is completely different from the so-called plasma crystal [20], which is caused by Coulomb crystallization in a dusty plasma. The latter plasma crystal may be used as a photonic crystal in the micrometer region, however, only with a few layers in the vertical direction and only for low-intensity light. The name *plasma photonic crystal* was originally introduced for a system of alternating thin plasma and dielectric material [21]. It can be realized, e.g., by arrays of periodic microplasmas instead of the arrays of dielectrics or metals in the conventional photonic crystals [22–27]. These plasma devices work in the microwave regime with low radiation intensity. For a TPPC, the plasma density gratings possess an ultrahigh damage threshold [28–31] which allows control of ultrashort intense laser pulses.

Crystal-lattice effects have been observed during short seed pulse amplification via backscattering instability in plasmas. One might distinguish two kinds of gratings that can be produced in plasma: One is based on stimulating an electron plasma wave (the Raman case) [32,33], and one is based on moving ions over a wavelength to make a neutralized density structure (the Brillouin case) [34–36]. The latter case, which is considered here, has rather different properties compared to the Raman case, both in transmitting light and in how long it lasts. Plasma density gratings induced by colliding laser fields inside a plasma volume were proposed for holography [32], an ion-ripple laser with intensities up to 10^{16} W/cm^2 [37], and compression of powerful x-ray pulses [33]. Overdense plasma gratings generated at the surface of initially plain solid targets play an important role in laser-matter interaction [38]. In all cases, the particle motion in the density gratings has to be analyzed carefully, since quite different aspects like dominating electron or ion motion, trapping, or stochastic motion might prevail [39]. Nonlinear effects may occur in the high-intensity relativistic regime [40].

The goal of the present Letter is to show that at the interface between laser-plasma physics and photonics new proposals for photonic crystals become possible. We present the main idea in two steps. First, we generate a TPPC by two oppositely propagating laser beams. The two laser pulses

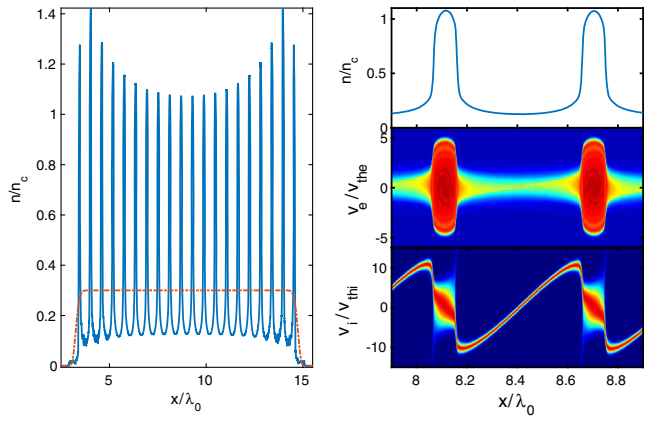

FIG. 1. Left: Electron density n/n_c at $t = 0$ (orange, dash-dotted line) and $t_2 = 1.25$ ps (blue line). Right: The electron density n/n_c (top), electron velocity (middle), and ion velocity (bottom) distributions, respectively, are shown at $t_2 = 1.25$ ps.

have vector potentials $\vec{A}_{1,2} = \frac{1}{2}A_{1,2}e^{i(\vec{k}_{1,2}\cdot\vec{r}-\omega_{1,2}t)}\vec{e}_y + \text{c.c.}$ with wave vectors $\vec{k}_2 = -\vec{k}_1$ and $\vec{k}_1 = k_1\vec{e}_x$. The laser frequencies are the same, i.e., $\omega_1 = \omega_2 \equiv \omega_0$. Within the plasma, the wave number k_1 is related to the vacuum wave number k_0 via $k_1 = k_0\sqrt{1 - n_0/n_c}$, where n_0 is the plasma background density and $n_c = \omega_0^2\epsilon_0 m_e/e^2$ is the critical plasma density. Here, m_e is the electron mass and ϵ_0 the vacuum dielectric constant. The two counterpropagating laser beams produce a zero frequency beat. By introducing the normalized vector potentials $a_{1,2} = eA_{1,2}/m_e c$, the ponderomotive force of the beat becomes $F_p = m_e c^2 a_1 a_2 k_1 \sin(2k_1 x)$. For linear polarization, the value of a corresponds to laser intensity I via $a = (7.3 \times 10^{-19} I[\text{W/cm}^2])^{1/2}\lambda[\mu\text{m}]$; λ is the laser wavelength.

Starting from an initially homogeneous plasma density n_0, the electrons will bunch within the ponderomotive troughs. The ponderomotive potential itself is too weak to act directly on the heavier species, but the space-charge field set up by the displaced electrons will act on the ions. By equating the ponderomotive force with the established electrostatic field, we obtain the estimate $E_{\max} = a_1 a_2\sqrt{1 - n_0/n_c}$ for the maximum space-charge field in terms of $E_0 = m_e c\omega_0/e$. The time scale for the ion reaction can be estimated from a two-fluid model as $t \approx [(m_i/m_e)/(k_1^2 c^2 a_1 a_2)]^{1/2}$ [37]. The initial velocity of the ions will be $v_i \sim c(m_e/m_i)E_{\max}t\omega_0$. In what follows, we consider an underdense electron-proton plasma with $m_i = 1836 m_e$ and $n_0 = 0.3 n_c$. The laser amplitude $a = a_1 = a_2 = 0.02$ is nonrelativistic, corresponding to about $I = 10^{15}$ W/cm^2 for $\lambda = 0.8$ μm. Then, the estimated response time of the ions becomes approximately 1 ps.

The self-consistent evolution of the plasma density in the presence of two counterpropagating laser pulses will be obtained from Maxwell-Vlasov simulations. Figure 1 shows results from a simulation where two multipicosecond flattop laser pulses interacted with a short plasma slab of initial electron (ion) temperature $T_e = 10$ eV ($T_i = 1$ eV).

On the left in Fig. 1, the electron density is shown at the two times $t = 0$ (initial distribution) and $t = 1.25$ ps (after entering the plasma). The simulations confirm the scenario of an initial dominance of the ponderomotive force on electrons and a subsequent streaking of the ions due to the space-charge field. At $t = 1.25$ ps, the spatial ion density distribution is almost the same as the spatial electron density distribution, meaning that the early time space-charge field has vanished already. We observe a strongly pronounced grating structure with very large peak values, reaching even overcritical densities. Within the troughs of the grating, the density has decreased to about $1/3$ of its initial value. The right side in Fig. 1 shows details at $t = 1.25$ ps, i.e., (electron or ion) density n, as well as electron and ion velocity distributions $f_{e,i}(x, v_x)$, for two grating periods around the center of the plasma slab. The density profile is very anharmonic, featuring an almost steplike profile alternating between $n_{\min} = 0.1 n_c$ and $n_{\max} = 1.1 n_c$. The phase space of the electrons shows very strong electron trapping inside the density peaks, leading to an almost flattop distribution function of width $\approx 5 v_{\text{the}}$, where $v_{\text{the}} = \sqrt{T_e/m_e}$ is the electron thermal velocity. After $t = 1.25$ ps, the ions still move ballistically. Because of their inertia, they traverse the peaks and move into the subsequent trough. At this time, the grating starts decaying.

When expanding the density in Fourier modes as

$$n(x) = \sum_p \eta_p e^{-i(2\pi/a)px}, \qquad \eta_p = \frac{1}{a}\int_0^a n(x)e^{i(2\pi/a)px}dx, \tag{1}$$

where $a = \pi/k_1$ is the period of the density grating, we obtain the time dependencies shown in Fig. 2.

The first four harmonics ($p = 1, 2, 3, 4$) of the density show the following. At about $t = 0.5$ ps, the nonlinear

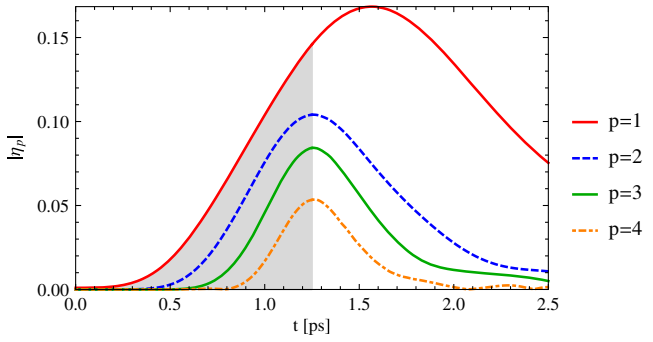

FIG. 2. Magnitude of the Fourier coefficients η_p, $p = 1, \ldots, 4$, of the plasma density, corresponding to the wave numbers $k_p = 2pk_0$, versus time. The shaded area designates the growth of the crystal.

phase of the density evolution sets in, driving subsequently the higher harmonics of the density modulation. At $t \approx 1$ ps, the density grating is fully developed. Subsequently, a decay due to the overshooting of the ions occurs with a characteristic time scale of picoseconds.

We will now analyze the photonic band structure caused by the fully established density grating. Later, we will discuss the oblique incidence of laser pulses onto the plasma. Hence, we have to take care of the polarization of the light. We focus on s polarization; the results for p polarization are, however, not fundamentally different. For s polarization, the wave equation for the transverse component of the electromagnetic wave is [41]

$$\left[\frac{\partial^2}{\partial x^2}+\frac{\partial^2}{\partial y^2}\right]E_z(\vec{r})+\frac{\omega^2}{c^2}\epsilon(x)E_z(\vec{r})=0, \tag{2}$$

where the dielectric function ϵ can be expressed as $\epsilon(x)=1-\omega_{pe}^2(x)/\omega_0^2$. Because of the structuring of the electron density n, the plasma frequency depends on x via $\omega_{pe}^2=n(x)e^2/\epsilon_0 m_e$. In order to solve (2), we make a Bloch wave ansatz

$$E_z(\vec{r})=\sum_{\vec{h}}c(\vec{h})e^{i(\vec{k}+\vec{h})\cdot\vec{r}}, \tag{3}$$

where $\vec{k}=(k_x,k_y)$. The lattice vector is $\vec{h}=(2\pi p/a,0)$, $p=0,\pm1,\pm2,\ldots$. Normalizing (2) by using $x_{\mathrm{unit}}=c/\omega_0=k_0^{-1}$ and $t_{\mathrm{unit}}=\omega_0^{-1}$, inserting (3), and setting the coefficient for the mode $\exp[i(k_x+2\pi p/a)x]$ to zero, we find the system of linear equations

$$c_p\left[-\left(k_x+\frac{2\pi}{a}\right)^2-k_y^2+\omega^2\right]-\sum_{p'}\eta_{p-p'}c_{p'}=0. \tag{4}$$

The roots of the determinant of (4) determine $\omega(\vec{k})$. For what follows, we truncate the system at $p=\pm3$, since we are interested in the lowest-order photonic band gaps; contributions by higher-order coefficients η_p, $p>\pm6$ to these gaps are marginal. The temporal variation of the coefficients η_p is directly reflected in the photonic band structure of the density grating.

In Fig. 3, we show the band structure for the first Brillouin zone (BZ) at two different times, $t_1=0.5$ ps and $t_2=1.25$ ps, respectively. At t_1, only the first harmonic η_1 contributes to $n(x)$; hence, we observe a band gap around ω_0 only at the border of the first BZ. Note that the border is located at $k_x/k_0=\sqrt{1-n_0/n_c}$ due to the wave number reduction in the plasma. The size of the gap is $\Delta\omega/\omega_0\hat{=}1.5\%$. With increasing time, $|\eta_1|$ grows substantially, resulting in a much wider band gap around ω_0, reaching $\Delta\omega/\omega_0\hat{=}15.2\%$ at t_2. At the same time, higher-order gaps appear due to the growth of $|\eta_2|,|\eta_3|,\ldots$, leading, for example, to a secondary gap around approximately $1.75\omega_0$ of $\Delta\omega/\omega_0\hat{=}5.3\%$. The width of the first

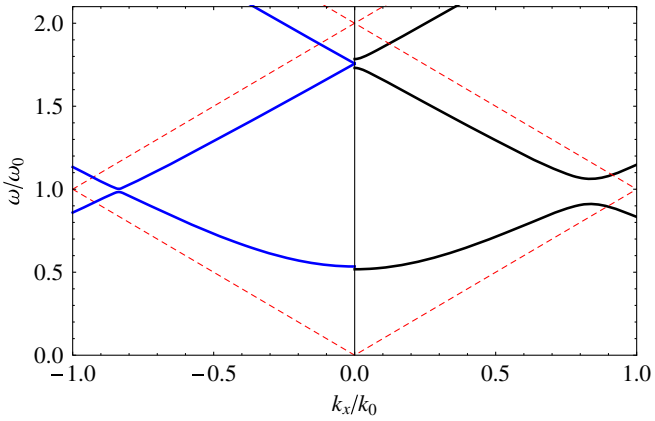

FIG. 3. Photonic band structure at $t=0.5$ ps (left, blue thick line) and $t=1.25$ ps (right, black thick line); the red dashed line corresponds to the light line $\omega=ck_x$. The first Brillouin zone ends at $k_1=k_0\sqrt{(1-n_0/n_c)}\approx0.83k_0$.

gap can be estimated by considering only the determinant of the 2×2 submatrix of (4) which couples the modes $p=0$ and $p=-1$. One obtains

$$\frac{\Delta\omega}{\omega_0}\approx2\left(1-\sqrt{\frac{\pi^2}{a^2}+\eta_0-\eta_{-1}}\right), \tag{5}$$

where $\eta_0=n_0$. Assuming a Gaussian pulse at 800 nm, the spectral bandwidth of the laser pulse can be estimated as $\Delta\omega/\omega_0=2.35/\tau$, where τ is the pulse duration at full width at half maximum of the electric field and is given in femtoseconds (fs). The grating may thus reflect pulses as short as about 15 fs in normal incidence at t_2.

For oblique incidence, we have $k_y\neq0$. Since a 1D TPPC is not structured along the y direction, k_y can attain any value. Figure 4 shows the photonic bands in dependence of k_y, where now continua of photonic modes exist due to the freedom $0\leq k_x\leq\pi/a$. Since $|\vec{k}|\geq k_y$ and all bands lie to the left of the light line $\omega=ck_y$, all TPPC modes are leaky modes and so can extend into the vacuum region. On the other hand, not all light incident onto the TPPC from the outside can penetrate into the TPPC, depending on the frequency ω_0 and the angle $\Theta=\mathrm{atan}(k_y/k_x)$. From Fig. 4, we deduce that the smallest angle for which the light of frequency ω_0 can penetrate into the plasma is $\Theta\approx25°$.

In the second step, we investigate the laser light pulse manipulation by the TPPC. For that, we conducted two-dimensional particle-in-cell (PIC) simulations using the EPOCH PIC code [42]. A 2D slab of plasma density $n_0=0.3n_c$, being homogeneous along y and initially confined to the region $-20\leq x\leq20$ μm, is considered. First, the plasma is irradiated by two counterpropagating Gaussian driver laser pulses of 500 fs FWHM duration. The pulses propagate along x and are assumed constant along y. The pulses initiate the formation of the density grating which persists after the pulses have left the plasma. About

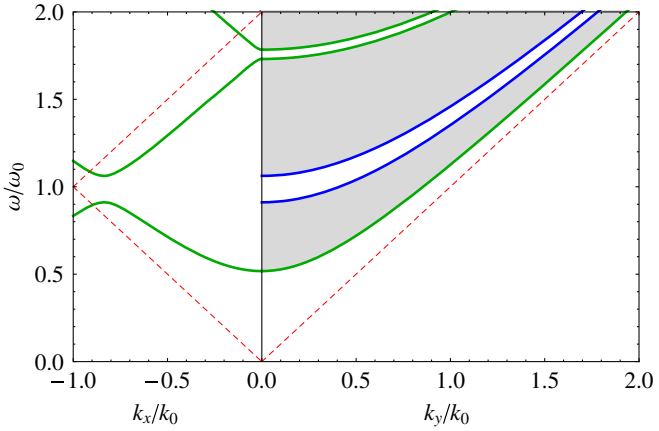

FIG. 4. Photonic band structure at $t = 1.25$ ps. On the left, we show for $-1 \leq k_x/k_0 \leq 0$ photonic bands for perpendicular incidence $\vec{k} = (k_x, 0)$ (green line) and vacuum light line $\omega = ck_x$. On the right, for $0 \leq k_y/k_0 \leq 2$ two superimposed band structures for $\vec{k} = (0, k_y)$ (green lines) and $\vec{k} = [(\pi/a), k_y]$ (blue lines) appear. The shaded region marks a continuum of bands at intermediate k_x. The red dashed line shows the light line $\omega = ck_y$.

0.5 ps after the driver pulses have left the plasma, we irradiate the plasma with a s-polarized 30 fs Gaussian probe pulse of intensity 10^{17} W/cm^2. The pulse is focused to an 8 μm diameter focal spot and incident at an oblique angle Θ. The probe and the driver pulses share the same wavelength $\lambda_0 = 800$ nm. At the time when the probe reaches the surface of the TPPC, the density profile is very similar to that shown in Fig. 1. Hence, for an interpretation of the probe pulse we can use the results presented in step one.

For angles up to $\Theta \approx 20°$, we find close to perfect reflectivity. Figure 5(a) shows the case $\Theta = 17°$, where the reflected pulse becomes slightly stretched. About 90% of the incident energy is reflected. At larger angles $\Theta \gtrsim 20°$, the TPPC begins to become transparent, as demonstrated in Fig. 5(b), where a pulse incident at $\Theta = 23°$ is propagating with almost no reflection through the plasma. The transmitted pulse has about 15% less energy than the incident pulse. The angular dependence of reflection and transmission agrees very well with the predictions from Fig. 4. The results from simulations for p polarization are similar to the s-polarization results shown here.

In the present Letter, we show results for 1D TPPCs. When using not exactly counterpropagating laser beams, one can generate 2D TPPCs. The structure of the 2D TPPCs resembles a square lattice of plasma rods. The angle between the driver pulses is an additional degree of freedom. It allows one to vary the lattice constants along the two directions. Evaluating the full 2D TPPC diversity, both in material properties and geometry of probe pulse incidence (see, e.g., Chapter 10 of Ref. [5] as well as the discussion of metamaterial properties in Ref. [43]), might open further applications of TPPCs.

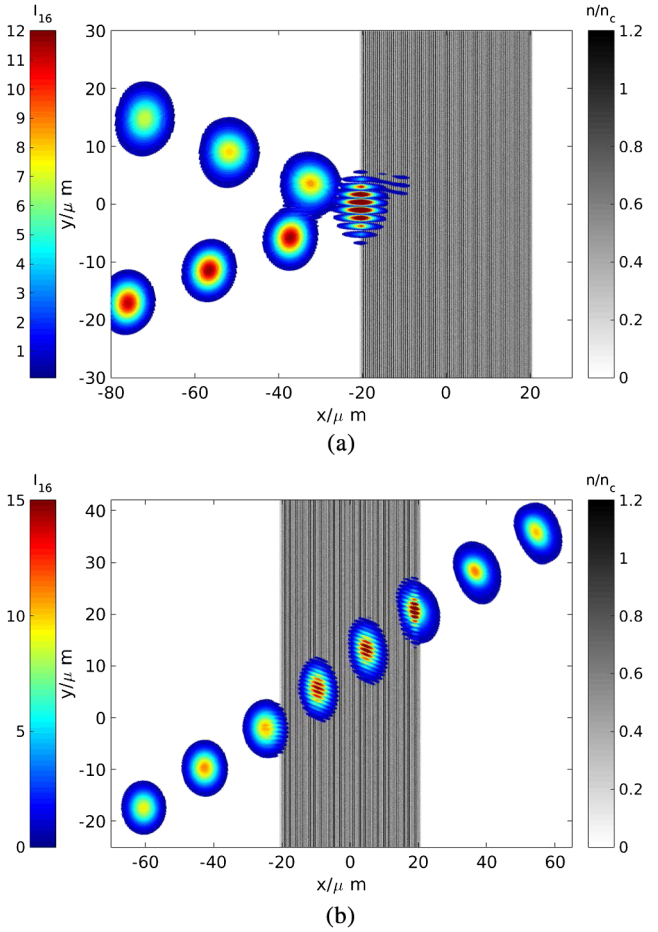

FIG. 5. Oblique incidence of a 30 fs s-polarized Gaussian laser pulse with a focal intensity of 10^{17} W/cm^2 and a focal spot size of 8 μm onto a TPPC. The incidence angles are (a) $\Theta = 17°$ and (b) $\Theta = 23°$, respectively. Shown is the laser intensity in units of 10^{16} W/cm^2 (in color) and the plasma density (as grayscale). A single laser pulse is shown at different times, starting at the lower left corner.

In conclusion, underdense plasma with crossed-laser beams can be utilized to manipulate optical signals in many ways. In contrast to the linear Raman regime with a plasma wave for recording and retrieving information [32], here we propose a density grating in the Brillouin regime, generating plasma photonic crystals for high-power lasers. The TPPC may act as a tunable mirror over a predictable time interval; it sustains intensities by orders of magnitude larger than what solid state photonic crystals can endure. Because of the large band gap, the TPPC operates for ultrashort pulses down to pulse durations of a few tens of femtoseconds. For the applicability of the linear photonic behavior, the ponderomotive force of the probe must not significantly affect the density distribution within the TPPC. Below the corresponding intensity limit, the reflection or transmission of high-power laser pulses can be predicted quite accurately by photonic band gap theory. At larger intensities, one might enter a weakly nonlinear

regime [9] with many new phenomena known under the topic "photonic crystals and nonlinearities"; see, e.g., Ref. [12]. Work is in progress to characterize and evaluate that regime. When damage of the TPPC starts, reflection may still take place, but the reflected pulse becomes distorted. However, when considering strong probe pulses with unwanted prepulses entering weak gratings, the prepulses may be reflected while the high-intensity main pulse will destroy the weak grating and propagate in the forward direction. Whether such a "cleaning" of pulses works in reality will be investigated in the future.

The work has been done under the auspices of the Sonderforschungsbereich TR18 of the DFG. The authors gratefully acknowledge the computing time granted by the John von Neumann Institute for Computing (NIC) and provided on the supercomputers JURECA at Jülich Supercomputing Centre (JSC). Further computational infrastructure was provided by the Centre for Information and Media Technology (ZIM) at the University of Düsseldorf. Development of the EPOCH PIC code was in part funded by the United Kingdom EPSRC Grants No. EP/G054950/1, No. EP/G056803/1, No. EP/G055165/1, and No. EP M022463/1.

[1] K. Ohtaka, Phys. Rev. B **19**, 5057 (1979).
[2] E. Yablonovitch, Phys. Rev. Lett. **58**, 2059 (1987).
[3] S. John, Phys. Rev. Lett. **58**, 2486 (1987).
[4] E. Yablonovitch and T. J. Gmitter, Phys. Rev. Lett. **63**, 1950 (1989).
[5] J. D. Joannopoulos, S. G. Johnson, J. N. Winn, and R. D. Meade, *Photonic Crystals: Molding the Flow of Light*, 2nd ed. (Princeton University, Princeton, NJ, 2008).
[6] Editorial, Taking things slow, Nat. Photonics **2**, 447 (2008).
[7] Editorial, Early lights: 25 years of photonic crystals, Nat. Mater. **11**, 995 (2012).
[8] T. Baba, Nat. Photonics **2**, 465 (2008).
[9] *Nonlinear Photonic Crystals*, edited by R. E. Slusher and B. J. Eggleton (Springer, New York, 2003).
[10] V. Berger, Phys. Rev. Lett. **81**, 4136 (1998).
[11] A. V. Andreev, A. V. Balakin, I. A. Ozheredov, A. P. Shkurinov, P. Masselin, G. Mouret, and D. Boucher, Phys. Rev. E **63**, 016602 (2000).
[12] *Photonic Crystals and Light Localization in the 21st Century*, edited by C. Soukoulis (Springer Science, New York, 2001).
[13] Y. S. Kivshar and G. P. Agrawal, *Optical Solitons: From Fibers to Photonic Crystals* (Academic, New York, 2003).
[14] D. Campbell, S. Flach, and Y. Kivshar, Phys. Today **57**, 43 (2004).
[15] F. Lederer, G. I. Stegeman, D. N. Christodoulides, G. Assanto, M. Segev, and Y. Silberberg, Phys. Rep. **463**, 1 (2008).
[16] H. S. Eisenberg, Y. Silberberg, R. Morandotti, and J. S. Aitchison, Phys. Rev. Lett. **85**, 1863 (2000).
[17] I. L. Garanovich, S. Longhi, A. A. Sukhorukov, and Y. S. Kivshar, Phys. Rep. **518**, 1 (2012).
[18] V. Shandarov, A. Perin, V. Ryabchenok, and F. Chen, in *Advanced Solid State Lasers* (Optical Society of America, Washington, DC, 2015), p. ATu2A.2.
[19] A.-C. Tien, S. Backus, H. Kapteyn, M. Murnane, and G. Mourou, Phys. Rev. Lett. **82**, 3883 (1999).
[20] H. Thomas, G. E. Morfill, V. Demmel, J. Goree, B. Feuerbacher, and D. Möhlmann, Phys. Rev. Lett. **73**, 652 (1994).
[21] H. Hojo and A. Mase, J. Plasma Fusion Res. **80**, 89 (2004).
[22] O. Sakai, T. Sakaguchi, and K. Tachibana, Appl. Phys. Lett. **87**, 241505 (2005).
[23] Y. Yin, H. Xu, M. Y. Yu, Y.-y. Ma, H.-b. Zhuo, C.-l. Tian, and F.-q. Shao, Phys. Plasmas **16**, 102103 (2009).
[24] B. Guo, Phys. Plasmas **16**, 043508 (2009).
[25] W. Fan, X. Zhang, and L. Dong, Phys. Plasmas **17**, 113501 (2010).
[26] L. Zhang and J.-T. Ouyang, Phys. Plasmas **21**, 103514 (2014).
[27] H.-F. Zhang, S.-B. Liu, and B.-X. Li, Phys. Plasmas **23**, 012105 (2016).
[28] M. Botton and A. Ron, Phys. Rev. Lett. **66**, 2468 (1991).
[29] P. Zhang, N. Saleh, S. Chen, Z. M. Sheng, and D. Umstadter, Phys. Rev. Lett. **91**, 225001 (2003).
[30] H. Wu, Z. Sheng, Q. Zhang, Y. Cang, and J. Zhang, Laser Part. Beams **23**, 417 (2005).
[31] P. Michel, L. Divol, D. Turnbull, and J. D. Moody, Phys. Rev. Lett. **113**, 205001 (2014).
[32] I. Y. Dodin and N. J. Fisch, Phys. Rev. Lett. **88**, 165001 (2002).
[33] V. M. Malkin and N. J. Fisch, Phys. Rev. Lett. **99**, 205001 (2007).
[34] A. A. Andreev, C. Riconda, V. T. Tikhonchuk, and S. Weber, Phys. Plasmas **13**, 053110 (2006).
[35] G. Lehmann and K. H. Spatschek, Phys. Plasmas **23**, 023107 (2016).
[36] L. Lancia, A. Giribono, L. Vassura, M. Chiaramello, C. Riconda, S. Weber, A. Castan, A. Chatelain, A. Frank, T. Gangolf, M. N. Quinn, J. Fuchs, and J.-R. Marquès, Phys. Rev. Lett. **116**, 075001 (2016).
[37] Z.-M. Sheng, J. Zhang, and D. Umstadter, Appl. Phys. B **77**, 673 (2003).
[38] S. Monchocé, S. Kahaly, A. Leblanc, L. Videau, P. Combis, F. Réau, D. Garzella, P. D'Oliveira, P. Martin, and F. Quéré, Phys. Rev. Lett. **112**, 145008 (2014).
[39] Z.-M. Sheng, K. Mima, Y. Sentoku, M. S. Jovanovic, T. Taguchi, J. Zhang, and J. Meyer-ter-Vehn, Phys. Rev. Lett. **88**, 055004 (2002).
[40] D. J. Stark, C. Bhattacharjee, A. V. Arefiev, T. Toncian, R. D. Hazeltine, and S. M. Mahajan, Phys. Rev. Lett. **115**, 025002 (2015).
[41] *Photonic Crystals*, edited by K. Inoue and K. Ohtaka (Springer, New York, 2004).
[42] T. D. Arber, K. Bennett, C. S. Brady, A. Lawrence-Douglas, M. G. Ramsay, N. J. Sircombe, P. Gillies, R. G. Evans, H. Schmitz, A. R. Bell, and C. P. Ridgers, Plasma Phys. Controlled Fusion **57**, 113001 (2015).
[43] D. R. Smith, J. B. Pendry, and M. C. K. Wiltshire, Science **305**, 788 (2004).